BJP BRITISH JOURNAL OF PHARMACOLOGY

BPS BRITISH PHARMACOLOGICAL SOCIETY

British Journal of Pharmacology (2009), 158, 588–600

0007-1188/09
www.brjpharmacol.org

RESEARCH PAPER

Metabolic characteristics of imatinib resistance in chronic myeloid leukaemia cells

Jelena Klawitter[1,2], Douglas J Kominsky[1,3], Jaimi L Brown[1], Jost Klawitter[1,2], Uwe Christians[1], Dieter Leibfritz[2], Junia V Melo[4], S Gail Eckhardt[3,5] and Natalie J Serkova[1,3,5]

[1]*Department of Anesthesiology, University of Colorado Health Sciences Center, Denver, CO, USA,* [2]*Department of Chemistry, University of Bremen, Bremen, Germany,* [3]*University of Colorado Cancer Center, University of Colorado Health Sciences Center, Denver, CO, USA,* [4]*Department of Hematology, Imperial College London, London, UK, and* [5]*Developmental Therapeutics and GI Malignancies Program, Division of Medical Oncology, Department of Medicine, University of Colorado Health Sciences Center, Denver, CO, USA*

Background and purpose: Early detection of resistance development is crucial for imatinib-based treatment in chronic myeloid leukaemia (CML) patients. We aimed to distinguish metabolic markers of cell resistance to imatinib.
Experimental approach: Two human imatinib-sensitive CML cell lines: LAMA84-s and K562-s, and their resistant counterparts: LAMA84-r and K562-r (both resistant to 1 μM imatinib), and K562-R (5 μM) were analysed by nuclear magnetic resonance spectroscopy to assess global metabolic profiling, including energy state, glucose and phospholipid metabolism.
Key results: We found, by Western blotting and flow cytometry, that the levels of Bcr-Abl tyrosine kinase and multi-drug resistance p-glycoprotein were inconsistent among resistant clones. On the other hand, phospholipid metabolism and lactate production were highly predictive for cell response to imatinib. As previously reported, sensitive cells showed significantly decreased glycolytic activity (lactate) and phospholipid synthesis (phosphocholine) as well as increased phospholipid catabolism (glycerophosphocholine) after 24 h of 1 μM imatinib treatment, which correlated with inhibition of cell proliferation and induction of apoptosis. In contrast to their sensitive counterparts, the K562-r, K562-R and LAMA84-r maintained increased phospholipid synthesis and glycolytic lactate production in the presence of 1 μM (K562-r and LAMA84-r) and 5 μM (K562-R) imatinib.
Conclusions and implications: Specific metabolic markers for early detection of imatinib resistance, including increased glycolytic activity and phospholipid turnover, can be identified in resistant clones. Once validated in human isolated leukocytes, they may be used to monitor the responsiveness of CML patients to treatment.
British Journal of Pharmacology (2009) **158,** 588–600; doi:10.1111/j.1476-5381.2009.00345.x; published online 6 August 2009

Keywords: imatinib resistance; cancer metabolomics; glycolysis; phospholipid metabolism; NMR spectroscopy; Bcr-Abl expression; drug-induced apoptosis; GLUT-1 transporter; Pgp expression

Abbreviations: CML, chronic myeloid leukaemia; FBS, fetal bovine serum; FITC, fluorescein isothiocyanate; G6PDH, glucose-6-phosphate dehydrogenase; GPC, glycerophosphocholine; GPT, D-glutamate-pyruvate transaminase; HK, hexokinase; LDH, lactate dehydrogenase; MS, mass spectrometry; NDP, nucleoside diphosphate; NMR, nuclear magnetic resonance; NTP, nucleoside triphosphate; PC, phosphocholine; PCA, perchloric acid; PCr, phosphocreatine; Pgp, p-glycoprotein; PI, propidium iodide; PtdCho, phosphatidylcholine; TCA, tricarboxylic acid; TSP, trimethylsilyl propionic acid

Introduction

Chronic myeloid leukaemia (CML) is a neoplasia of haematopoietic cells generated by the *BCR-ABL* fusion gene, the molecular product of the (9;22)(q34;q11) chromosomal translocation. *BCR-ABL* encodes a p210 oncoprotein with constitutively active cytoplasmic tyrosine kinase that does not block differentiation, but enhances proliferation and viability of myeloid cells (Deininger *et al.*, 2000).

Imatinib mesylate is an Abl tyrosine kinase inhibitor of 2-phenylamino pyrimidines, which acts by competitively inhibiting ATP binding to the Abl kinase domain (Buchdunger *et al.*, 1996; Druker *et al.*, 1996). Its binding abrogates the activity of the Bcr-Abl oncoprotein through inhibition of Bcr-Abl autophosphorylation and substrate phosphorylation,

Correspondence: Natalie J Serkova, University of Colorado Health Sciences Center, 12631 East 17th Avenue, AO1, Aurora, CO 80045, USA. E-mail: Natalie.Serkova@ucdenver.edu
Received 28 March 2009; revised 30 March 2009; accepted 31 March 2009

leading to suppression of cell proliferation and induction of apoptosis (Druker *et al.*, 1996; Deininger *et al.*, 1997; Gambacorti-Passerini *et al.*, 1997). Imatinib also possesses inhibitory properties against other members of the tyrosine kinase family such as platelet-derived growth factor receptor and c-kit (Buchdunger *et al.*, 2000). The only known curative treatment for CML, to date, is allogenic bone marrow transplantation from histocompatible donors, but the procedure is associated with a high risk of morbidity and mortality. Imatinib is able to control CML in the majority of the patients, but primary or secondary resistance to the inhibitor is matter of concern (Gorre *et al.*, 2001; Melo and Chuah, 2007).

The most frequent mechanism of imatinib resistance in Bcr-Abl transformed cells is the emergence of a sub-clone of cells with mutations in the Abl kinase domain (Melo and Chuah, 2007). Point mutations can directly prevent the binding of imatinib to the Bcr-Abl protein or can lead to conformational changes of the kinase, affecting binding of the inhibitor in an indirect way (Roche-Lestienne *et al.*, 2002). Resistance to imatinib can also be caused by Bcr-Abl overexpression due to amplification of the *BCR-ABL* gene, as originally described in the LAMA84-r and AR230-r cell lines (le Coutre *et al.*, 2000; Van Etten, 2004). Like most other small molecules, imatinib needs to pass through the cell membrane to reach its target protein. For many such compounds, transmembrane proteins, which are involved in drug influx into or efflux from the cell, have been implicated in mediating drug resistance, and there is evidence that imatinib is also a substrate and/or inhibitor of transporter proteins (Mahon *et al.*, 2000; Thomas *et al.*, 2004; Jordanides *et al.*, 2006).

Although the correlation between the molecular mechanisms and imatinib efficacy/resistance in clinical trials is well established, their link to the metabolic consequences of imatinib treatment is still unknown. It has been shown that Bcr-Abl-positive cells express the high-affinity GLUT-1 glucose transporter and have increased glucose uptake (Boros *et al.*, 2002; Serkova and Boros, 2005). Furthermore, recent studies showed that the control of glucose-substrate flux is an important mechanism of the anti-proliferative action of imatinib, and imatinib-sensitive cells have decreased glycolytic activity while maintaining mitochondrial homeostasis (Boren *et al.*, 2001; Gottschalk *et al.*, 2004). On the other hand, choline phospholipid metabolism is altered in a wide variety of cancers, including blood cancers (Franks *et al.*, 2002; Gottschalk *et al.*, 2004; Glunde and Serkova, 2006). An elevation of phosphocholine (PC), the major phospholipid precursor, was observed in diseased leukocytes isolated from chronic lymphocytic leukaemia patients when compared with normal leukocytes (Franks *et al.*, 2002). Finally, energy metabolism is highly sensitive to the anti-cancer treatment especially during the induction of apoptosis (Evelhoch *et al.*, 2000; Gottschalk *et al.*, 2004). The aim of the present study was to assess the global metabolic profiling of imatinib-resistant and sensitive human CML cells and to establish metabolic indicators of imatinib resistance. Oncogenesis-related metabolic pathways, such as phospholipid from the Kennedy pathway, glucose and energy metabolism (Warburg' effect) were assessed and linked to cell proliferation and apoptosis in imatinib-resistant CML cells. Finally, we determined the expression of the efflux transport p-glycoprotein (Pgp) and the intracellular imatinib concentration in sensitive cells versus resistant cells.

Methods

Cell cultures and imatinib treatment

Two imatinib-sensitive CML cell lines, K562-s and LAMA84-s, as well as their resistant counterparts K562-r and LAMA84-r cell lines (resistant to 1 μM imatinib) were generated as previously described (Mahon *et al.*, 2000). In K562-r, cells are resistant due to impaired Bcr-Abl autophosphorylation; in LAMA84-r cells the up-regulation of Bcr-Abl and imatinib transporting Pgp were discussed as possible mechanisms of cells resistance to imatinib (Mahon *et al.*, 2000). The third resistant cell line, K562-R (resistant to 5 μM imatinib) was a generous gift. In contrast to K562-r cells (resistant to 1 μM imatinib), the resistance of K562-R cells has been shown to be independent of Bcr-Abl expression and signalling, and may be mediated in part through overexpression of other tyrosine kinases such as src-related LYN kinase (Donato *et al.*, 2003).

All cells were grown in RPMI 1640 culture medium containing 10% fetal bovine serum (FBS). The cells were kept at 37°C with 95% air/5% CO_2. The sensitive K562-s and LAMA84-s cells were treated with 1 μM imatinib for 24 h. The resistant cells were constantly grown in the presence of 1 μM (K562-r and LAMA84-r) or 5 μM imatinib (K562-R cells).

Cell proliferation and viability were examined by cell counting using a cell counter and trypan blue exclusion respectively.

Cell extraction for nuclear magnetic resonance (NMR) spectroscopy

For NMR experiments, the cells were incubated with 5 mM [1-^{13}C]-glucose for 4 h before perchloric acid (PCA) extraction. All cell extractions were performed using a previously published PCA extraction protocol allowing for water-soluble and lipid fraction separation (Gottschalk *et al.*, 2004). Lyophilized media and water-soluble cell extracts were re-dissolved in 1.5 and 0.5 mL of deuterium oxide respectively. After centrifugation, the supernatants were neutralized to pH 7.2 to allow precise chemical shift assignments. Lipid extracts were re-dissolved in 1 mL mixture of deuterated methanol/chloroform (2:1, v/v).

NMR spectroscopy

High-resolution ^{1}H- and ^{13}C-NMR experiments were performed with the Bruker 500 MHz DRX spectrometer equipped with an inverse 5 mm TXI probe and ^{31}P-NMR experiments with the 300 MHz Bruker Avance system with a 5 mm QNP probe. For proton NMR, a standard water presaturation pulse programme was used for water suppression; spectra were obtained at 12 ppm spectral width, 32 K data arrays, 64 scans with 90 degree pulses applied every 12.8 s. Trimethylsilyl propionic-2,2,3,3,-d_4 acid (TSP, 0.5 mM) was used as an external standard for metabolite chemical shift assignment (0 ppm) and quantification (for exact metabolite assignment

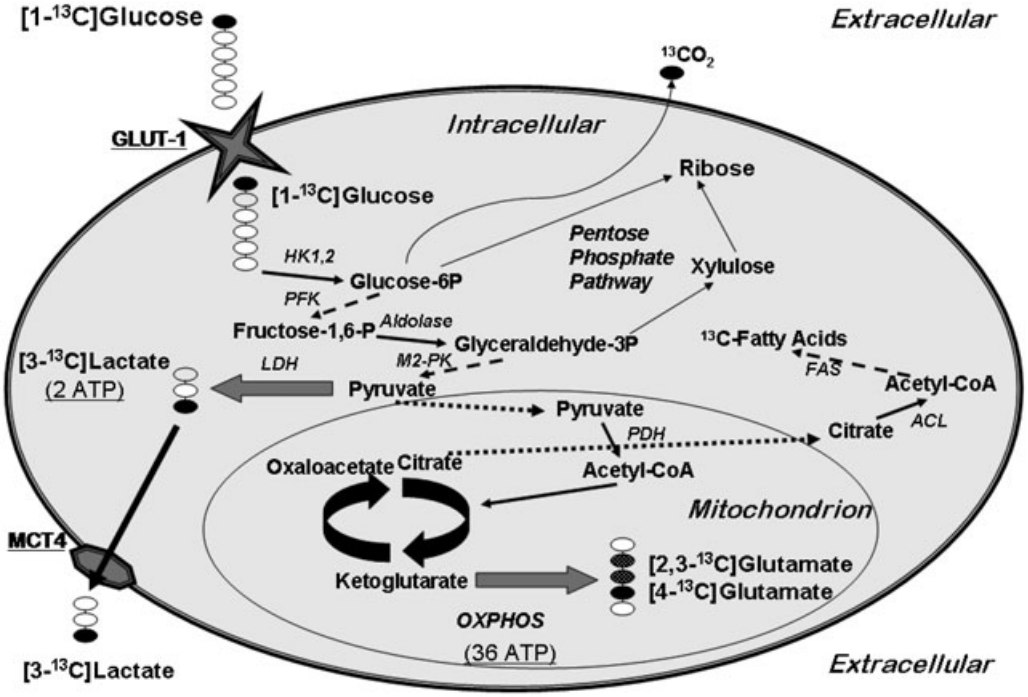

Figure 1 Metabolic fate of the ^{13}C-label from [1-^{13}C]-glucose. Label incorporation (black solid circles) is presented for glycolytic and tricarboxylic acid (TCA) cycle intermediates from metabolism of [1-^{13}C]-glucose. Briefly, in cancer cells, increased uptake of [1-^{13}C]-glucose through the glucose transporter GLUT-1 is detected by analysing extracellular levels of [1-^{13}C]-glucose in the media. Increased activity of glycolysis was calculated from the amount of intracellular [3-^{13}C]-lactate in the cellular fraction, as well as the amount of lactate exported into media through the monocarboxylate transporter (MCT4). Decreased mitochondrial activity is detected by low levels of ^{13}C-enrichment into [4-^{13}C]-glutamate (and glutamine, through pyruvate dehydrogenase) and [2,3-^{13}C]-glutamate (and glutamine, through pyruvate carboxylase from the first TCA run). Finally, exported acetyl-CoA (from the truncated TCA cycle) into the cytosol is used for increased ^{13}C-fatty acid synthesis. ^{13}C-fluxes through the pentose phosphate pathway can be detected by alternative methods such as GC-LC.

and their chemical shifts refer to Serkova *et al*. (2005). ^{13}C-NMR spectra with proton decoupling were recorded using the C3-lactate peak at 21 ppm as chemical shift reference (spectral width was 150 ppm, 16 K data arrays, 20 K scans applied every 3 s). For quantification of absolute concentrations of ^{13}C-metabolites, the possible positions for ^{13}C-labelling of the metabolite of glycolysis or the tricarboxylic acid (TCA) cycle after incubation of cells with [1-^{13}C]-glucose were determined according to the chart on Figure 1. [3-^{13}C]-lactate satellite peak (at 1.23 ppm) from ^{1}H-NMR spectra served as an internal standard for ^{13}C-NMR spectra (at 21 ppm) for calculation of ^{13}C-enrichment of glucose and glucose metabolites (Zwingmann and Leibfritz, 2003; Gottschalk *et al*., 2004). In order to confirm that ^{13}C-NMR-based calculations of *de novo* [1-^{13}C]-glucose uptake and metabolism are correct, we also performed standard enzymatic analysis on the same medium spectra (see below). ^{31}P-NMR spectra were obtained using the spectral width of 50 ppm and 16 K data arrays, with 6–10 K scans being applied every 3.5 s. Before the ^{31}P-NMR spectra were recorded, EDTA (100 mM) was added to each PCA extract to complex divalent cations. Methylene diphosphonic acid (2 mM) was used as an external standard for chemical shift references (18.6 ppm) and for metabolite quantification in ^{31}P-NMR. All data were processed using the Bruker WINNMR programme. All NMR experiments were performed at the Metabolomics NMR University of Colorado Cancer Center Core.

Enzymatic analysis of glucose and lactate concentrations in media

To cross-validate ^{13}C-NMR analysis on *de novo* ^{13}C-metabolite fluxes, D-glucose and L-lactate concentrations in cell media were determined using their respective Megazyme assay kits. The assays were run according to the manufacturer's protocols. Briefly, for glucose studies 170 µL water, 10 µL imidazole buffer, 10 µL ($NADP^+$/ATP) solution and 8 µL of collected medium were mixed together and the absorbance read after 2–3 min. The reaction was started by addition of 2 µL hexokinase (HK, 425 U·mL^{-1}) plus glucose-6-phosphate dehydrogenase (G6PDH, 212 U·mL^{-1}):

$$\text{glucose} + \text{ATP} \rightarrow \text{glucose-6-phosphate} + \text{ADP (by HK)},$$

$$\text{glucose-6-phosphate} + \text{NADP}^+ \rightarrow \text{gluconate-6-phosphate} + \text{NADPH} + \text{H}^+ \text{ (by G6PDH)}.$$

The absorbances were read again after 5–20 min and the concentration of glucose was calculated as follows:

$$c = (V * M_w)/(\varepsilon * d * v) * \Delta A_{Glucose}$$

where V: final volume (mL); M_w: molecular weight of glucose (g·mol^{-1}); ε: extinction coefficient of NADPH at 340 nm (6300 L·mol^{-1}·cm^{-1}); d: light path (cm) and v: sample volume (mL).

For lactate studies 128 μL water, 50 μL glycylglycine buffer, 10 μL NAD^+, 2 μL D-glutamate-pyruvate transaminase (GPT, 1000 U·mL^{-1}) and 8 μL of collected medium were mixed together and the absorbance read after 2–3 min. The reaction was started by addition of 2 μL lactate dehydrogenase (LDH, 2000 U·mL^{-1}):

$$\text{lactate} + NAD^+ \rightarrow \text{pyruvate} + NADH + H^+ \text{ (by LDH)},$$

$$\text{pyruvate} + \text{glutamate} \rightarrow \text{alanine} + \text{2-oxoglutarate (by GPT)}.$$

The absorbances were read again after 10–30 min, and the concentrations of lactate were calculated based on the equation above for calculation of glucose concentration [where M_w: molecular weight of lactate (g·mol^{-1})].

HPLC-MS/MS (mass spectrometry) analysis for quantification of phosphate metabolites

For the additional nucleotide concentration measurements, an Agilent 1100 high-performance liquid chromatography (HPLC) system coupled to a mass selective detector via an electrospray ionization interface was used (Klawitter *et al*., 2007). The cells (10^7 cells) were extracted using the PCA extraction protocol (see above) and analysed using the validated HPLC/MS method. After the lyophilisates had been dissolved in 500 μL water, 20–40 μL sample were injected into an HPLC system equipped with an online desalting column. The range of reliable response of the assay was 10–1000 pmol nucleotides on column using N6-(aminohexyl)-adenosine-5′3′-diphosphate as an internal standard. Ions were recorded in the negative single ion monitoring mode: AMP (m/z = 346), ADP (m/z = 426), ATO (m/z = 506), GDP (m/z = 442), GTP (m/z = 522), UDP (m/z = 403), UTP (m/z = 483), CDP (m/z = 402), CTP (m/z = 482), NAD (m/z = 662), FAD (m/z = 784). Day-to-day accuracy was 100–112%, and total imprecision of the assay was 2.8–15.1%. After dilution integrity had been successfully established, cell extracts were diluted 1:5 so that the measured concentration would be positioned within the range of reliable response.

Quantification of intracellular *and extracellular imatinib concentrations by LC/MS/MS*

Intracellular and extracellular imatinib concentrations were determined using a fully validated LC/MS/MS assay (Klawitter *et al*., 2009). The cells (10^7 cells) were frozen in liquid nitrogen and resuspended in 800 μL methanol/0.2 M zinc sulphate (7:3, v/v) solution, which was spiked with the internal standard trazodone (2 ng·mL^{-1}). After the samples had been vortexed and subjected to ultrasonic treatment for 10 min, they were centrifuged (1300× *g*, 10 min, +4°C), and the supernatants were injected into the HPLC system for online extraction. After activation of the column switching-valve the extracts were back-flushed onto the analytical column (Luna, C18, 50·4.6mm, 5 μm). The HPLC system interfaced with a triple stage quadrupole MS (API4000) was run in positive multiple reaction monitoring mode. Peak area ratios obtained from multiple reaction monitoring mode of the mass transition for imatinib (m/z 494.5→394.2) and the internal standard trazadone (m/z 372.5→176.4) were used for quantification. The lower limit of quantification was 0.03 ng·mL^{-1}, and the assay was linear between 0.03 and 75 ng·mL^{-1}. No matrix interferences, carry-over or relevant ion suppression were detected. Day-to-day accuracy was 93.1–114.1%, and total imprecision of the assay was 3.1–13.2%. Samples could undergo three freeze/thaw cycles, and the extracted samples were stable in the autosampler at +4°C for at least 24 h.

Western blot assays

Cellular phosphotyrosine content and inhibition of kinase activity was assessed by Western blot analysis. Protein lysates were electrophoresed on 7% SDS-PAGE gels and transferred to polyvinylidene difluoride membranes by semidry electrophoretic transfer. The membrane was blocked with 3% dry milk and 0.1% Tween 20 in phosphate-buffered saline (PBS) and incubated with primary antibodies (4G10 anti-phosphotyrosine and β-actin). The filters were washed and incubated with horseradish peroxidase-conjugated donkey anti-rabbit antibody, and the ratios of specific phosphorylated protein to β-actin bands were determined by densitometry.

Flow cytometry analysis

In order to compare protein expression levels, the cells were washed, fixed, permeabilized and stained with the following primary antibodies: anti-Abl (1:50 dilution for 45 min incubation times), anti-phosphotyrosine (4G10, 1:50 dilution for 30 min incubation times) and anti-Pgp (MRK16, 1:25 dilution for 120 min incubation times). The following protocols were used: for fixation, 10^7 cells were collected and washed with PBS. The cells were resuspended in 5 mL freshly prepared methanol-free formaldehyde (2% in PBS). The fixation was carried out at 37°C for 15 min. The cells were centrifuged and washed again in 5 mL ice-cold PBS. In the next step, permeabilization, 90% ice-cold methanol (10 mL for final concentrations of 10^6 cells·mL^{-1}) were added to the cell pellet, vortexed and kept on ice for 30 min. One millilitre of cell suspension was centrifuged with FACS buffer (0.5% bovine serum albumin in PBS). The cells were incubated with FACS buffer for 20 min (room temperature) and resuspended, centrifuged again, and resuspended with 100 μL primary antibody (for dilutions and incubation times see above). Primary antibody solution was removed and cells soaked in FACS buffer for 30 min, followed by addition of 100 μL secondary FITC (fluorescein isothiocyanate)-conjugated goat anti-rabbit IgG antibody (1:50 dilution) to the cell pellet. The resuspended cells were incubated in the dark for 45 min. Another washing and soaking in FACS buffer step followed, with final cell resuspension in 500 μL FACS buffer for flow cytometry analysis. The mean fluorescence intensity (x-mean all) of control and treated cells was used for the quantification of protein expression.

For measurements of apoptosis and necrosis, cells were incubated with YoPro-1 and propidium iodide (PI) dyes. Cells were centrifuged at 300× *g* for 10 min, washed in PBS and resuspended in RPMI media without Phenol red with final concentrations of 10^6 cells·mL^{-1}. Following staining with 0.1 μM YoPro-1 and 1 μg of PI per millilitre, the cells were

incubated for 30 min on ice and subsequently analysed by flow cytometry with FL1@530 nm- and FL2@575 nm-compensated emission readings.

All flow cytometry analyses were performed on Becton Dickinson FACSCalibur or Beckman Coulter FC500 at the Flow Cytometry Core Facility, UCDHSC, Denver, CO (under the supervision of Dr K Helm and Mr M Ashton).

Statistical analysis

All experiments were repeated at least four times. All numerical data are presented as mean ± SD from the replicate experiments. One-way analysis of variance (ANOVA) method was used to determine differences between groups (untreated sensitive vs. treated sensitive vs. resistant). Tukey's test was used as a *post hoc* test in combination with ANOVA to test for significances between groups. The significance level was set at $P < 0.05$ for all tests (SigmaPlot-version 9.01, Systat Software, Point Richmond, CA, USA and SPSS version 14.0, SPSS Inc., Chicago, IL, USA).

Materials

RPMI 1640 culture medium containing 10% FBS were obtained from Invitrogen Co. (Carlsbad, CA, USA); K562-R was a generous gift from Dr Talpaz (MD Anderson Center, Houston, TX, USA); imatinib was kindly provided by Dr Buchdunger (Novartis Pharmaceuticals, Basel, Switzerland); cell counter, Beckman (Fullerton, CA, USA); [1-^{13}C]-glucose, Cambridge Isotope Laboratories (Andover, MA, USA); spectrometer equipped with an inverse 5 mm TXI probe Bruker BioSpin (Fremont, CA, USA); Megazyme assay kits, Megazyme International Ireland Ltd. (Co. Wicklow, Ireland, UK); Agilent 1100 HPLC, mass selective detector and electrospray ionization interface, Agilent Technologies (Palo Alto, CA, USA); N6-(aminohexyl)-adenosine-5′3′-diphosphate and trazodone, Sigma-Aldrich (St Louis, MO, USA); analytical column (Luna, C18, 50·4.6mm, 5 μm) Phenomenex (Torrance, CA, USA); triple stage quadrupole MS, API4000, Applied Biosystems (Foster City, CA, USA); 4G10 anti-phosphotyrosine and β-actin, Santa Cruz Biotechnology (Santa Cruz, CA, USA); anti-Abl, Cell Signaling Technology, Inc. (Beverly, MA, USA); anti-phosphotyrosine (4G10), Santa Cruz Biotechnology; anti-Pgp (MRK1), Alexis Biochemicals (San Diego, CA, USA); FITC-conjugated goat anti-rabbit IgG antibody, Amersham Biosciences (Piscataway, NJ, USA); YoPro-1 and PI dyes, Molecular probes (Eugene, OR, USA).

Results

Cell proliferation and viability

Treatment with 1 μM imatinib induced almost complete inhibition of cell proliferation in both sensitive cell lines, K562-s and LAMA84-s (Figure 2A). Not only cell proliferation, but also cell viability was decreased with only 65% K562-s and 55% LAMA84-s viable cells being detected after 48 h of imatinib treatment (Figures 2A and 3C). In contrast, cell proliferation rate of all three resistant cell lines, K562-r (5 μM, 1 μM) and LAMA84-r (1 μM) was only slightly, but not significantly decreased (Figures 2B and 3C). The presence of imatinib did not affect cell viability in K562-r or LAMA84-r.

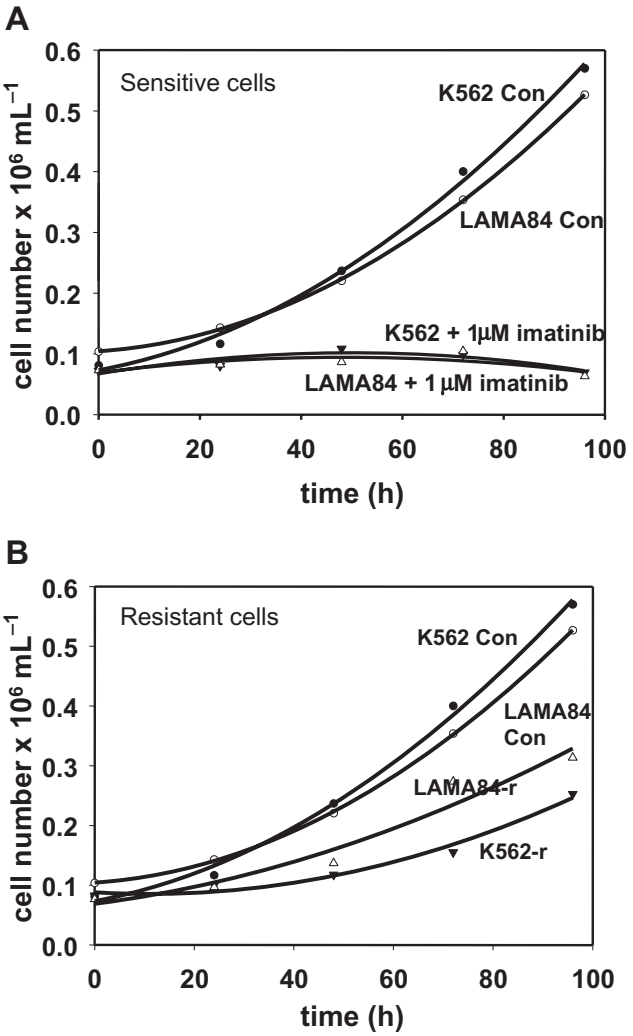

Figure 2 Cell proliferation curves for human Bcr-Abl-positive K562 and LAMA84 cells. (A) Untreated sensitive cells (control) and sensitive cells treated with 1 μM imatinib; (B) untreated sensitive cells (control) and resistant cells grown in the presence of 1 μM and 5 μM imatinib. The cells were counted immediately after seeding (0 h), and after 24, 48, 72 and 96 h (each time point $n = 3$). To facilitate visual comparison, proliferation curves in (B) were presented without ±SD (see Figure 3C for mean and SD values).

Cell apoptosis

If untreated, most of the K562-s and LAMA84-s cells were viable (bottom left corner) without significant signs of apoptosis (Figure 4A). After 24 h of treatment with 1 μM imatinib, apoptosis was observed in a significantly higher proportion of sensitive cells: 18% ($P < 0.005$) in LAMA84-s and 27% ($P < 0.005$) in K562-s cells (Figures 3D and 4B). No significant changes in the induction of apoptosis or necrosis were detected in resistant cell lines compared with their sensitive counterparts (Figures 3D and 4C). In all experiments, necrosis

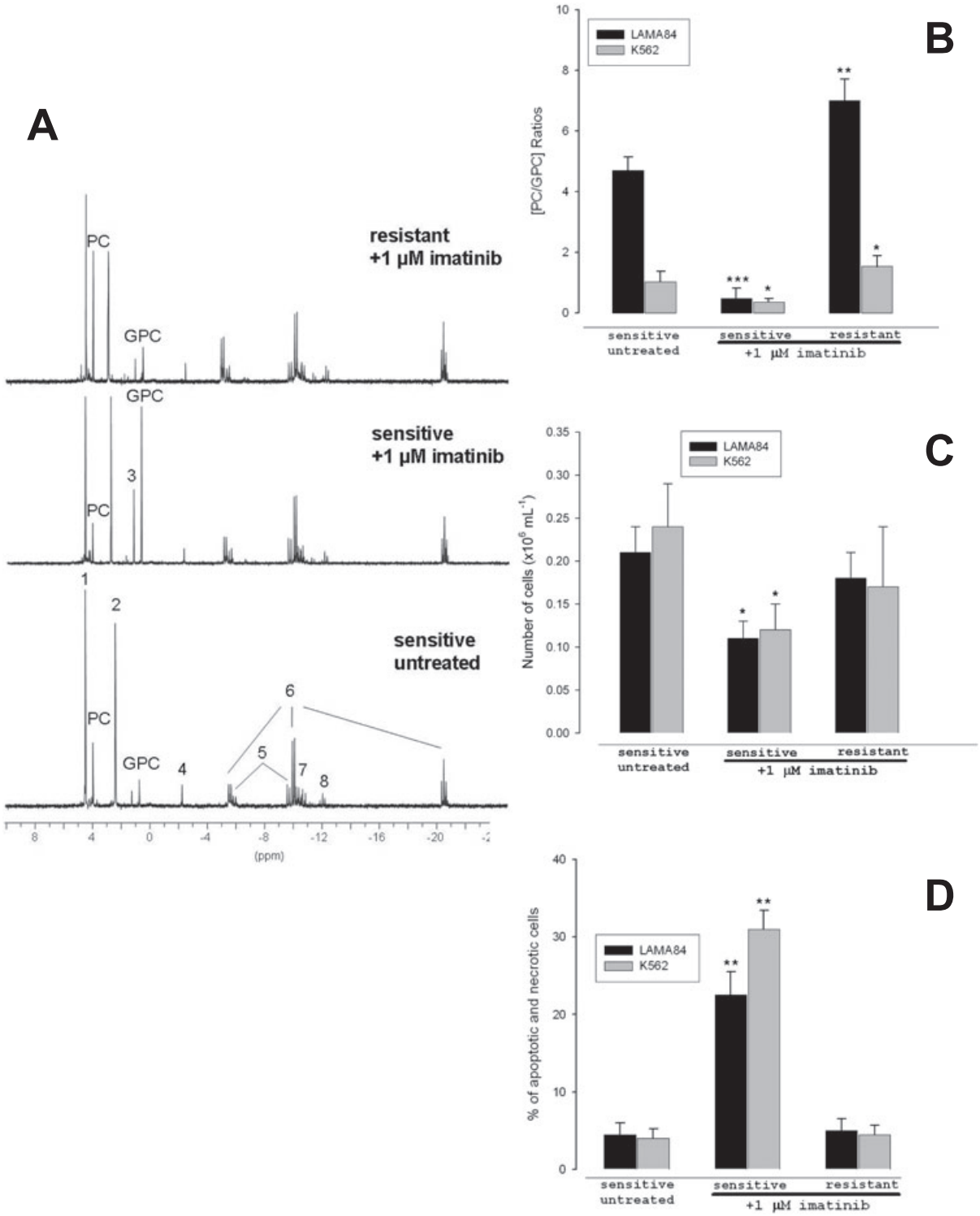

Figure 3 (A) Representative ^{31}P-NMR spectra of LAMA84 cell extracts with and without imatinib treatment. (B) The ratios PC/GPC, calculated from ^{31}P-NMR spectra of LAMA84 and K562 cell extracts, reflect the synthesis-to-degradation proportion in phospholipid metabolism, correlate with cell proliferation (C) and inversely correlate with apoptosis induction (D). K562- and LAMA84-sensitive cells were treated with 1 µM imatinib for 24 h and compared with their 1 µM imatinib-resistant counterparts (K562-r and LAMA84-r). All data are presented as mean ± SD ($n = 4$) with statistical significance *$P < 0.05$, **$P < 0.005$ and ***$P < 0.001$. GPC, glycerophosphocholine; NMR, nuclear magnetic resonance; PC, phosphocholine. NMR peak assignment: 1, phosphoethanolamine; 2, inorganic phosphate, 3, glycerophosphoethanolamine; 4, phosphocreatine; 5, nucleotide diphosphates; 6, nucleotide triphosphates; 7, sugar phosphates and NAD$^+$; 8, sugar phosphates alone.

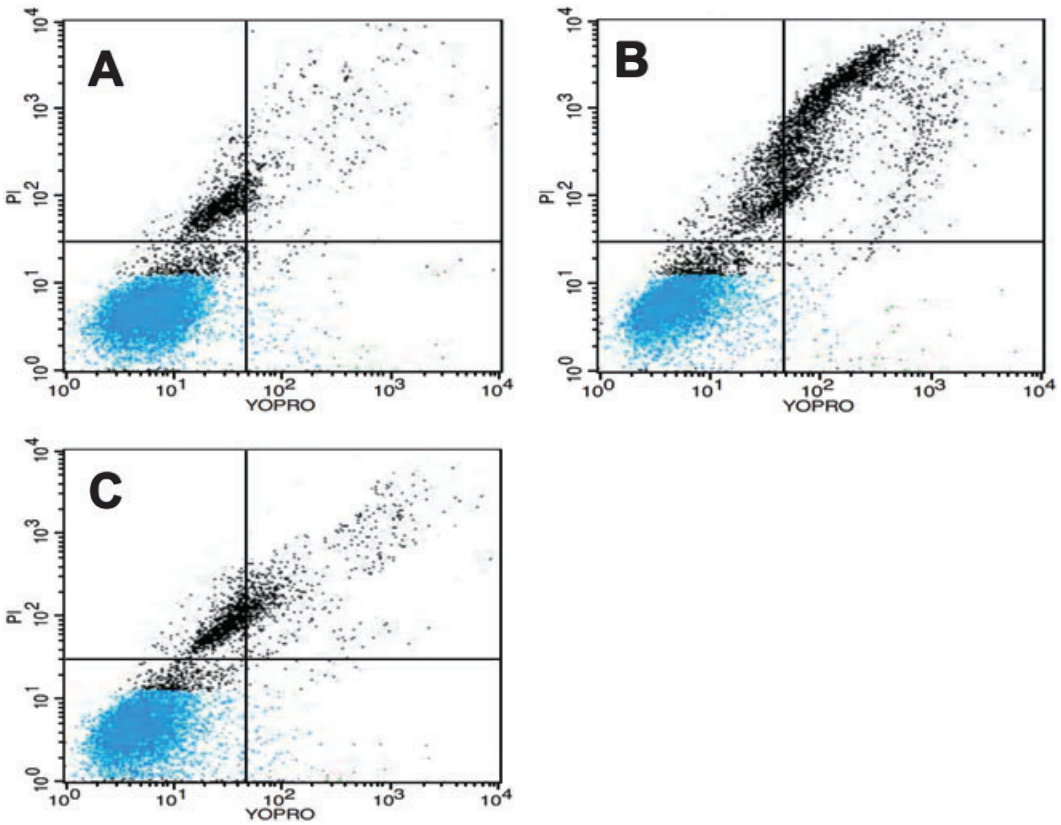

Figure 4 Flow cytometry plots of K562 cells: (A) untreated sensitive cells (control); (B) sensitive cells treated with 1 μM imatinib for 24 h; and (C) resistant cells in the presence of 1 μM imatinib ($n = 4$ for each group). In each plot, four quadrants with different cell viabilities were distinguished: bottom left, live; upper left, necrotic; bottom right, early apoptotic; upper right, apoptotic cells. After the staining with YoPro and propidium iodide (PI), the living cells (bottom left corner) were non-fluorescent by flow cytometry, while having the ability to exclude both dyes. Early apoptotic cells, which were labelled with YoPro, but still maintained the ability to exclude PI, were located in the bottom right corner. Finally, apoptotic (upper right corner) and necrotic (upper left corner) cells were both YoPro- and PI-positive. Hence, live cells are non-fluorescent, early apoptotic cells YoPro-positive only and late apoptotic and necrotic cells are both YoPro-positive and PI-positive (upper two quadrants in the plot). In all cultures 3–6% necrotic cells were observed due to the staining procedures. Prior to flow cytometry analysis, fluorescence microscopy experiments using Annexin V-fluorescein isothiocyanate (Annexin-FITC) had been carried out for qualitative assessment of apoptosis (not quantitative) to confirm YoPro flow cytometry data.

was observed in 3–6% of the cell population due to the staining procedure.

Changes in phospholipid metabolism

The major difference in the metabolic profile in sensitive (imatinib-treated) versus resistant cells, detected by ^{31}P-NMR, was a significant change in PC concentrations, the major precursor for membrane phospholipids (Table 1, Figure 3A). In sensitive cells, the treatment with 1 μM imatinib for 24 h significantly decreased PC concentrations (45% of control in K562-s and 72% in LAMA84-s cells, Table 1); this paralleled the inhibition of cell proliferation (Figure 3B and C). The decrease in PC was followed by a decrease in phosphatidylcholine (PtdCho, the major membrane phospholipid) in lipid fractions. Its signal decreased to 58% in K562-s and to 73% in LAMA84-s cells treated with imatinib. In contrast to sensitive treated cells, no decrease in PC and PtdCho concentrations was found in either K562-r (1 μM) or K562-R (5 μM) cells compared with untreated K562-s cells (Table 1). Moreover, LAMA84-r cells showed markedly increased PC and PtdCho concentrations (260% and 137% of control, respectively, Table 1 and Figure 3A). Maintenance of high levels of phospholipid synthesis in the resistant cells reflects the high proliferation rate of these cells (Figure 3B and C).

Another significant hallmark of imatinib sensitivity revealed by ^{31}P-NMR was an increase in phosphodiester signals, such as glycerophosphocholine (GPC) and glycerophosphoethanolamine (GPE), which are the degradation products of membrane phospholipids. Both GPC and GPE concentrations were greatly increased in LAMA84-s and K562-s cells after the 24 h incubation with 1μM imatinib, when compared with untreated cells (Table 1, Figure 3A). Increased catabolism of membrane phospholipids revealed increased apoptotic processes in sensitive cells treated with imatinib (Figure 3D). As a consequence, the ratios of PC/GPC were markedly decreased in sensitive, imatinib-treated cells (Table 1, Figures 3B). In contrast, all three resistant cell lines showed an increased PC/GPC ratio compared with untreated sensitive counterparts and even more so when compared with treated sensitive cells (Table 1, Figure 3B) while maintaining the high proliferation rate (Figure 3C) and suppressed levels of apoptosis (Figure 3D).

Table 1 Concentrations (nmol·g^{-1} wet weight) of high-energy phosphates (PCr, NTP, NDP), phospholipids (PC, GPC and PtdCho) and their ratios (in italics) calculated from LAMA84 (A) and K562 (B) cell extracts and lipids using ^{1}H- and ^{31}P-NMR and HPLC/MS

	A			*B*			
	LAMA84-s	*LAMA84-s + 1 μM*	*LAMA84-r (1 μM)*	*K562-s*	*K562-s + 1 μM*	*K562-r (1 μM)*	*K562-R (5 μM)*
PCr	173 ± 62	126 ± 69*	154 ± 57	514 ± 129	217 ± 77**	n.d.	189 ± 65***
NTP	1795 ± 519	1630 ± 160	2368 ± 240*	3138 ± 746	2154 ± 260	2309 ± 71*	1764 ± 45**
NDP	570 ± 103	650 ± 251	585 ± 74	439 ± 124	375 ± 84	458 ± 42	347 ± 29*
Energy balance	*3.17 ± 0.86*	*2.51 ± 0.80*	*4.06 ± 0.40**	*7.15 ± 1.19*	*5.72 ± 1.02*	*5.07 ± 0.34**	*5.11 ± 0.45**
Energy charge	*0.64 ± 0.10*	*0.56 ± 0.06*	*0.90 ± 0.02**	*0.63 ± 0.08*	*0.56 ± 0.13*	*0.42 ± 0.06***	*0.48 ± 0.11**
PtdCho	2793 ± 509	2045 ± 494*	3828 ± 862*	2347 ± 626	1354 ± 659*	2740 ± 91	2749 ± 860
PC	576 ± 250	414 ± 187*	1492 ± 252***	959 ± 101	436 ± 124**	777 ± 72	877 ± 136
GPC	122 ± 34	861 ± 217***	322 ± 66*	945 ± 196	1256 ± 150*	506 ± 106*	505.6 ± 86.3**
PC/GPC	*4.71 ± 0.44*	*0.48 ± 0.33****	*7.00 ± 0.72***	*1.02 ± 0.37*	*0.35 ± 0.13**	*1.53 ± 0.35**	*1.73 ± 0.41**

Values are presented as means ± SD of 4–6 independent experiments.
Significance levels: *$P < 0.05$; **$P < 0.005$; ***$P < 0.001$, were determined by ANOVA (with *post hoc* pair-wise multiple comparison Tukey's test).
GPC, glycerophosphocholine; MS, mass spectrometry; n.d., not detectable; NDP, nucleoside diphosphate; NMR, nuclear magnetic resonance; NTP, nucleoside triphosphate; PC, Phosphocholine; PCr, phosphocreatine; PtdCho, phosphatidylcholine.

Table 2 Concentrations of ^{13}C-labelled endogenous metabolites (nmol·g^{-1} cell wet weight) in LAMA84 and K562 cell extracts as calculated from ^{13}C-NMR spectra (Figure 1)

	[3-^{13}C]-lactate, intracellular and extracellular	*[4-^{13}C]-glutamate*	*[3-^{13}C]-lactate ratio [2,3,4-^{13}C]-(Glu + Gln)*
LAMA84-s, untreated	2376 ± 662	2534 ± 50	9.31 ± 1.21
LAMA84-s + 1 μM (24 h)	1731 ± 104*	164 ± 32*	9.68 ± 1.33
LAMA84-r (1 μM)	4108 ± 219**	363 ± 88*	11.51 ± 0.48*
K562-s, untreated	2277 ± 329	330 ± 63	7.03 ± 0.63
K562-s + 1 μM (24 h)	1322 ± 247**	188 ± 73*	6.31 ± 0.52*
K562-r (1 μM)	2137 ± 790	230 ± 82	9.02 ± 1.08**
K562-R (5 μM)	2219 ± 499	257 ± 13	8.76 ± 0.76*

Results are given as mean ± SD ($n = 6$).
Significance levels: *$P < 0.05$; **$P < 0.005$, were determined by ANOVA (with *post hoc* pair-wise multiple comparison Tukey's test).
NMR, nuclear magnetic resonance; Gln, glutamine; Glu, glutamate.

In addition, a significant increase in the synthesis of all lipids, including polyunsaturated fatty acids (PUFA: 269%, $P < 0.005$, $n = 6$) and cholesterol (167%, $P < 0.05$, $n = 6$) was observed in K562-s (and to a lesser extent in LAMA84-s) cells after imatinib treatment. No changes in lipid metabolism were seen in resistant cells when compared with untreated sensitive cells.

Energy state after imatinib treatment

Loss of cell vitality and induction of apoptosis usually leads to a decreased energy state in the cell. The concentrations of high-energy phosphates – phosphocreatine, nucleoside triphosphates (NTP) and nucleoside diphosphates (NDP) – were determined in cell extracts by ^{31}P-NMR spectroscopy (Figure 3A) and/or HPLC/MS. Surprisingly, the treatment with 1 μM imatinib did not result in significant decrease in the energy state of sensitive cells. The energy balance calculated as the NTP/NDP ratio, slightly decreased, but this was not significant, in the K562-s and LAMA84-s cells treated with 1 μM imatinib (Table 1). Accordingly, no significant changes were found in UTP/UDP and GTP/GDP ratios or in the energy charge (ATP + 0.5ADP)/(ATP + ADP + AMP) as assessed by HPLC/MS (Table 1). However, the concentration of phosphocreatine, which had previously been shown to decrease faster than ATP during apoptotic processes, substantially decreased to 53% and 65% of control in K562-s- and LAMA84-s-treated cells respectively (Table 1).

In contrast to persistent phospholipid alterations, there was no consistency in the high-energy changes among resistant cell lines. In both K562-r (1 μM) and K562-R (5 μM imatinib resistance) cells, phosphocreatine and NTP levels as well as the energy balance decreased as compared with K562-s cells (Table 1). The energy charge also decreased to 67% in K562-r (1 μM) and to 76% in K562-R (5 μM) (Table 1). In contrast, in LAMA84-r cells the energy balance increased to 128% and the energy charge to 141% of control ($P < 0.05$, Table 1).

Mitochondrial metabolism and glycolysis

After incubation with 1 μM imatinib and [1-^{13}C] glucose, both energy producing pathways – cytosolic glycolysis (3-^{13}C-lactate production) and mitochondrial TCA cycle (2,3,4,-^{13}C-glutamate and glutamine, see chart on Figure 1) – were down-regulated in the sensitive cells. As revealed by ^{13}C-NMR, imatinib strongly inhibited glycolytic activity of sensitive cells: production of [3-^{13}C]-lactate (after addition of intracellular and extracellular concentrations) decreased to 58% in K562-s and 71% in LAMA84-s cells ($P < 0.05$, Table 2). The ^{13}C-enrichment into the mitochondrial TCA cycle activity was

Table 3 Intracellular concentrations of imatinib in sensitive and resistant (r: cells resistant to 1 μM and R: cells resistant to 5 μM imatinib) Bcr-Abl-positive cells as measured using HPLC-MS/MS assay

	4 h treatment	*24 h treatment*
LAMA84-s + 1 μM imatinib	55.8 ± 3.9	58.5 ± 2.1
LAMA84-r	37.2 ± 1.9*	36.6 ± 0.6*
K562-s + 1 μM imatinib	71.7 ± 2.2	87.5 ± 2.6
K562-r	56.1 ± 0.3*	56.5 ± 0.9**
K562-s + 5 μM imatinib	155.1 ± 2.1	166.5 ± 3.8
K562-R	147.2 ± 5.7	161.0 ± 8.3

The data are presented as nM per 10^7 cells. Results are given as mean ± SD ($n = 5$).
No imatinib was detected in sensitive, untreated cell lines.
Significance levels: *$P < 0.005$; **$P < 0.001$, were determined by ANOVA (with *post hoc* pair-wise multiple comparison Tukey's test) for time point paired sensitive versus resistant cells.

also equally reduced by 1 μM imatinib; [4-^{13}C]-glutamate decreased to 57% of K562-s and 66% of LAMA84-s cells ($P < 0.05$, Table 2). The relative activity of cytosolic glycolysis to mitochondrial TCA cycle [3-^{13}C-lactate/2,3,4-^{13}C-(glutamate + glutamine) ratios] did not change in LAMA84-s, but was significantly decreased in K562-s cells ($P < 0.05$, Table 2), indicating a specific inhibition of aerobic glycolysis in imatinib-treated sensitive cells.

In contrast to the sensitive cells, imatinib failed to inhibit glycolytic activity in all three resistant cell lines. Moreover, the glycolytic activity was even elevated in LAMA84-r cells when compared with untreated controls: 3-^{13}C-lactate was 173% of that in untreated LAMA84-s cells ($P < 0.005$, Table 2). The changes in the mitochondrial TCA cycle were inconsistent among resistant cell lines. LAMA84-r cells had a slightly increased 4-^{13}C-glutamate production rate while both K562 resistant cell lines (K562-r and K562-R) had a slightly lower mitochondrial activity compared with controls (Table 2). This explains the higher energy levels in LAMA84-r cells, while both K562-r and K562-R cell lines had decreased energy levels.

Intracellular imatinib concentrations

The intracellular imatinib concentrations were measured in sensitive cell lines over the time–course of the experiments. Intracellular imatinib concentrations after 4 h of treatment with 1 μM imatinib were 55.8 nM per 10^7 LAMA84-s cells and 72.0 nM per 10^7 K562-s cells. Only a slight, insignificant increase in intracellular imatinib accumulation was observed after 24 h of treatment, when compared with 4 h (Table 3). The intracellular drug concentrations in all 1 μM resistant cells were significantly lower than in their sensitive counterparts treated with 1 μM imatinib (62% for LAMA84-r and 55% for K562-r of sensitive treated cells, $P < 0.05$, $n = 5$).

Interestingly, the intracellular imatinib concentrations in K562-s cells treated with 5 μM imatinib were only twofold higher then after 1 μM imatinib treatment (155.0 nM vs. 72.0 nM per 10^7 K562-s cells after 4 h; Table 3). Because the final concentration calculated as a sum of intracellular and extracellular (media) concentrations was as expected (1 μM and 5 μM, respectively), an analytical error was excluded, and saturation for transport processes could occur at high (5 μM) imatinib doses. Again, no significant changes in intracellular imatinib distribution were observed between 4 and 24 h after imatinib treatment.

No significant differences in imatinib cell accumulation were observed between K562-s treated with 5 μM imatinib and resistant K562-R (5 μM).

Expression of the Pgp multi-drug resistance protein

Three resistant cell lines showed inconsistent changes in the expression levels of multi-drug resistance Pgp when compared with their sensitive counterparts. The resistant LAMA84-r cells significantly overexpressed the Pgp, as revealed by flow cytometry analysis [Figure 5A and B; in accordance with the results of Mahon *et al*. (2000)]. The K562-r, resistant to 1 μM imatinib, showed only a slight increase in Pgp expression (Figure 5C and D), while K562-R (5 μM) cells had no detectable changes in Pgp (in accordance with the findings of Donato *et al*., 2003, data not shown). Treatment with 1 μM imatinib for 24 h resulted in a slight, but not significant decrease of Pgp expression in both sensitive cell lines (data not shown). Increased expression of the Pgp efflux transporters partly explains the lower intracellular drug concentrations in LAMA84-r versus LAMA84-s cells, treated with 1 μM imatinib.

Bcr-Abl expression and phosphorylation

Because the LAMA84-s cell line does not contain a normal ABL gene, the level of Bcr-Abl expression in LAMA84 cells was examined by flow cytometry of permeabilized cells with an anti-Abl mAb (Figure 6A). When treated with 1 μM imatinib, LAMA84-s cells showed a twofold increase in Bcr-Abl protein level compared with their sensitive control ($P < 0.05$, Figure 6B), while the changes in K562-s cells did not reach statistical significance (data not shown). In LAMA84-r cells the level of expression was 10-fold higher compared with LAMA84-s ($P < 0.0005$, Figure 6C). Confirming previous results from our co-investigator's laboratories, the K562-r 1 μM cell line did not show an increase in Bcr-Abl protein expression (Mahon *et al*., 2000), while the K562-R 5 μM cells had reduced Bcr-Abl expression (Donato *et al*., 2003) (data not shown).

Because imatinib specifically reduces the tyrosine kinase activity of Bcr-Abl, we also confirmed its effect on the level of tyrosine phosphorylation, known from previous findings (Mahon *et al*., 2000; Donato *et al*., 2003). Incubation with 1 μM imatinib reduced the fluorescence intensity of p-tyr staining by Western blot as well as flow cytometry analysis, to non-detectable levels in both LAMA84-s and K562-s cell lines (Figure 6D). The resistant cells revealed no changes in p-tyr phosphorylation (Mahon *et al*., 2000; Donato *et al*., 2003) (data not shown).

Discussion

In the present study, we identified the metabolic pathways implicated in responsiveness to imatinib treatment in human Bcr-Abl-positive cells with differential sensitivity to imatinib.

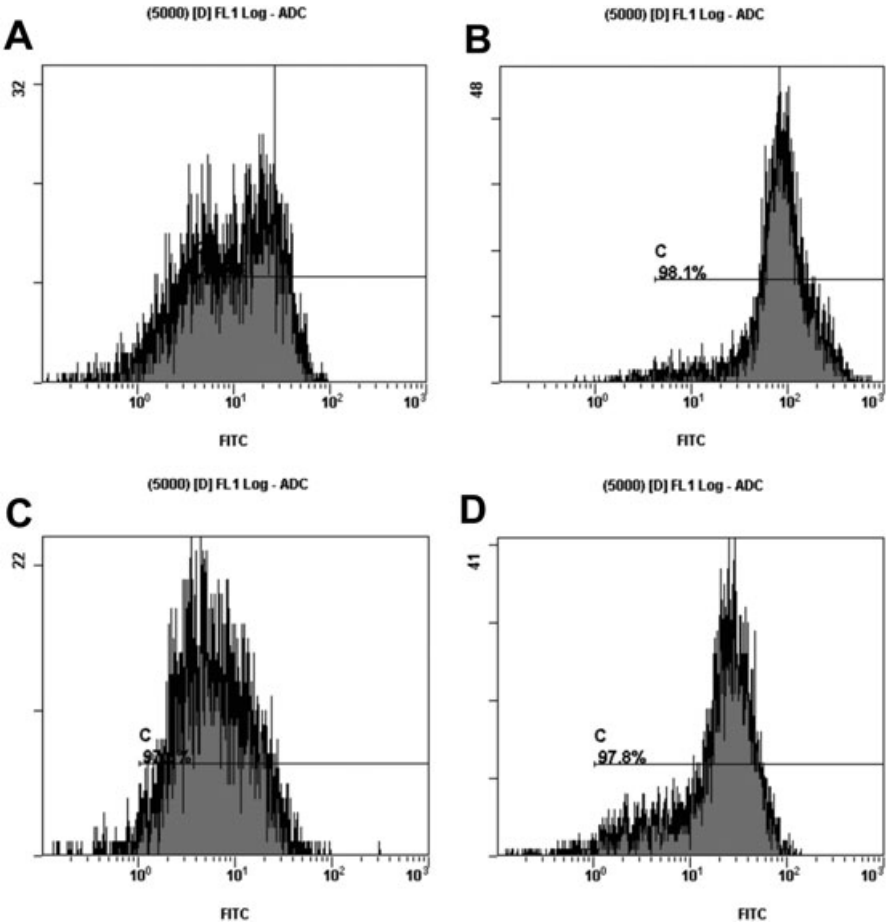

Figure 5 Flow cytometry plots of P-glycoprotein expression in (A) LAMA84-s-untreated and (B) LAMA84-r cells; (C) K562-s-untreated and (D) K562-r (1 μM) cells. FITC, fluorescein isothiocyanate.

Three well-established imatinib-resistant cell lines were used for the studies. Involvement of Bcr-Abl protein expression and/or its autophosphorylation has been discussed as a possible mechanism of resistance in both to 1 μM imatinib-resistant cell lines LAMA84-r and K562-r (Mahon *et al.*, 2000; Desplat *et al.*, 2005). The resistance occurrence in K562-R cell line resistant to 5 μM imatinib has been shown to be independent of Bcr-Abl expression and signalling and may be mediated in part through overexpression of other tyrosine kinases such as src-related LYN kinase (Donato *et al.*, 2003; Wu *et al.*, 2008). While no consistent molecular markers were found among three resistant lines, two distinguished metabolic pathways (among others) were identified in all three resistant clones, namely increased glycolysis (Warburg' effect) and increased phospholipid turnover (Kennedy biosynthesis pathway and phospholipase-mediated breakdown pathways for phospholipids).

Metabolic differences among imatinib-responsive and resistant cells were correlated with the rates of cell proliferation, apoptosis induction, Pgp expression and intracellular imatinib concentrations. Imatinib-sensitive K562-s and LAMA84-s cells showed significantly decreased synthesis and increased catabolism of phospholipids after 24 h of 1 μM imatinib treatment, which correlated well with inhibition of cell proliferation and induction of apoptosis respectively. Significant decreases in glucose metabolism, especially highly decreased glycolytic activity in treated sensitive cells, revealed cell-specific metabolic responses to inhibition of cell proliferation and induction of apoptosis. In contrast to their sensitive counterparts, the resistant cells, despite the presence of 1 μM imatinib, maintained proliferation, did not undergo apoptosis, had elevated phospholipid synthesis and maintained a highly glycolytic phenotype. In addition, two resistant cell lines revealed significantly lower intracellular concentrations of imatinib, with high Pgp levels being partly responsible.

Expression of the oncoprotein Bcr-Abl is an important initial step in leukaemogenesis in CML. The discovery of the specific Bcr-Abl tyrosine kinase inhibitor, imatinib, has started a new era of targeted cancer therapy (Buchdunger *et al.*, 1996). Despite its highly specific mechanism of action, development of resistance to imatinib treatment occurs in patients. Therefore, reliable markers that can predict early development of resistance to imatinib are in demand. Previously, Gottschalk *et al.* (2004) and more recently Barnes *et al.* (2005) showed that the inhibition of Bcr-Abl activity by imatinib in K562 cells caused significant changes in cellular glucose metabolism. Bcr-Abl-positive cells express the high-affinity GLUT-1 glucose transporter and possess high glucose uptake. Therefore, effects of imatinib on glucose flux and cell

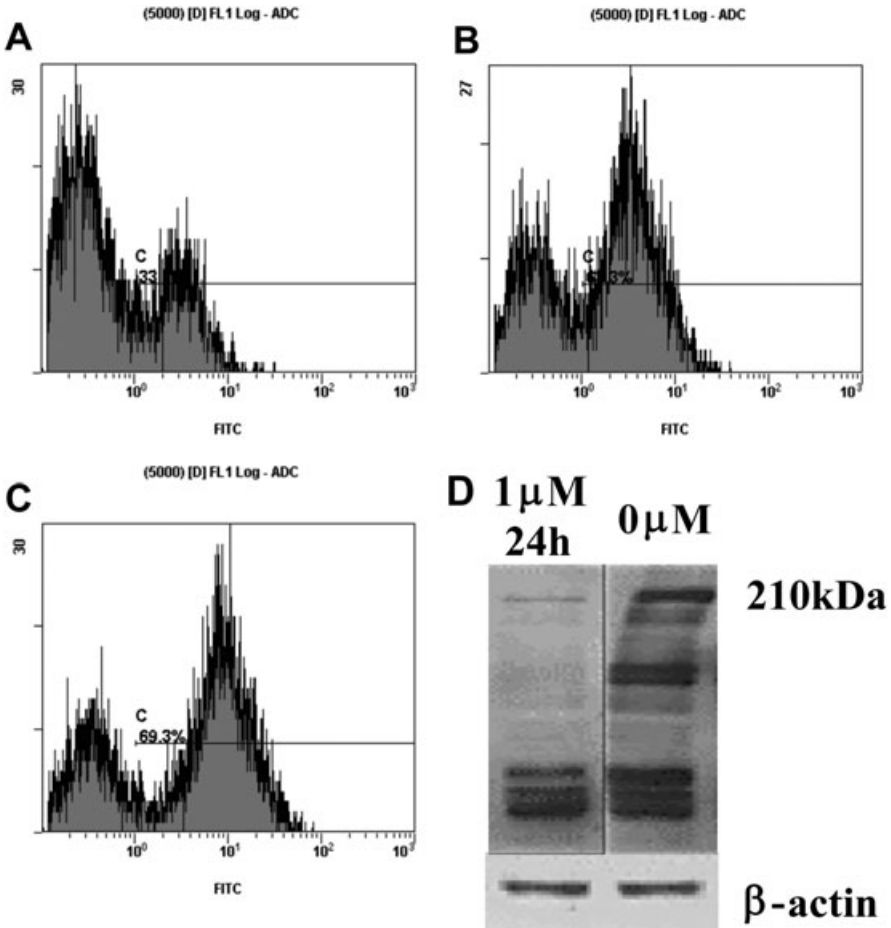

Figure 6 Flow cytometry analysis of human BCR-ABL-positive LAMA84 cell lines for Abl expression in (A) LAMA84-s-untreated, (B) LAMA84-s-treated with 1 μM imatinib (24 h), (C) LAMA84-r cells resistant to 1 μM imatinib. (D) Phosphorylation of Bcr-Abl in LAMA-s (with and without imatinib) cells. All experiments were repeated; $n = 4$ for each group. FITC, fluorescein isothiocyanate.

metabolism are important in understanding the resulting cell changes, ranging from apoptosis to resistance development. It has also been proposed that imatinib treatment may restrict *de novo* nucleic acid and fatty acid synthesis by inducing a significant decrease in HK and glucose-6-phosphate-1-dehydrogenase activity and altering pathway carbon flux through the pentose cycle (Boren *et al.*, 2001; Serkova and Boros, 2005). On the other hand, the metabolic profile of tumours, including leukaemias, is also characterized by an elevation of membrane biosynthesis and, therefore, elevated choline phospholipid metabolism (Franks *et al.*, 2002; Glunde and Serkova, 2006; Morse *et al.*, 2009). NMR spectroscopy can be used to detect these metabolic changes as endogenous biomarkers of cancer, or as surrogate markers for monitoring tumour response to novel targeted therapies. Therefore, we aimed to evaluate the qualitative and quantitative changes occurring in the metabolic pathways of imatinib-sensitive versus imatinib-resistant cell lines.

The most sensitive and consistent marker that differentiated the metabolic signatures of cell responsiveness versus resistance to imatinib was phospholipid metabolism. The main membrane phospholipid, PtdCho and its major biosynthetic precursor, PC are known to be increased in all rapidly proliferating malignant cells including leukaemia cells (Franks *et al.*, 2002) due to overexpression of the key enzymes choline kinase (Kennedy biosynthetic pathway) and phospholipase A2 (phospholipid catabolism, mostly in inflammation-associated cancers) (Glunde and Serkova, 2006; Morse *et al.*, 2009). In both sensitive lines, K562-s and LAMA84-s, decreased concentrations of PC and PtdCho were observed after imatinib treatment and correlated with the inhibition of cell proliferation. In addition, the products of phospholipid degradation, such as GPC and -ethanolamine, were greatly increased after imatinib treatment in these cells. This was associated with induction of the apoptotic cell death processes. The PC/GPC ratios were markedly decreased in sensitive cell lines as a consequence of imatinib treatment. In contrast, the resistant counterparts maintained a high proliferation rate and high rates of phospholipid synthesis. The proliferating resistant cells did not exhibit apoptotic activity and showed significantly higher PC/GPC ratios compared with the untreated sensitive cells (Figure 3B–D).

Induction of apoptosis is known to induce changes in the energy state of the cell – both ATP depletion as well as ATP increase have been observed previously (Evelhoch *et al.*, 2000; Zamaraeva *et al.*, 2005). Such variability in ATP levels might, at least in part, be attributed to differences in the time period of apoptotic stimulation and/or the degree of contamination

by cells that have already died and lost ATP. During the induction phase of apoptosis cells can still maintain a high level of ATP, which is necessary for the increased fatty acid biosynthesis (Henke *et al*., 1999). In the present study, sensitive treated cells, with obvious signs of apoptosis, revealed a slight, but not statistically significant, decrease in their energy state. At the same time, imatinib-treated cells had increased fatty acid biosynthesis. The resistant counterparts grown in 1 μM imatinib did not show any impairment in their energy state. Thus, in contrast to distinguished changes in choline phospholipid metabolism, imatinib (a first cytostatic agent approved for clinical use) has no significant effect on cell energy production, the major metabolic target for cytotoxic drugs. The resistant clones also maintained metabolic homeostasis and compensated for the increased energy demands due to their high proliferation rates. Therefore, the energy state of the cells does not predict their sensitivity to imatinib.

Glucose consumption is directly related to energy production in cells. Cancer cells are highly dependent on aerobic glycolysis to compensate for their high demands of ATP due to increased proliferation rates – the Warburg' effect (Warburg, 1956). Significant differences in glucose metabolism were observed upon imatinib treatment. Glycolysis rate in K562-s and LAMA84-s cells, treated with imatinib, was decreased due to the decreased proliferation rate, therefore less [3-^{13}C]-lactate was produced. Simultaneously, the decrease in [4-^{13}C]-glutamate production from [1-^{13}C]-glucose in the presence of 1 μM imatinib indicated decreased glucose metabolism through the mitochondrial TCA cycle. In a previous study, an increase in mitochondrial activity and energy balance was observed when cells were treated with lower concentrations of imatinib (0.25 μM) for 96 h (Gottschalk *et al*., 2004). In contrast, the resistant cells maintained an elevated glycolysis and lactate production. High glucose uptake to support increased activity of glycolytic enzymes is one of the most important hallmarks of oncogenesis (Zhou *et al*., 2002). Most recently, it has been shown that increased glycolysis in fast proliferating cells is directly controlled by major signal transduction pathways involved in oncogenesis. In solid tumours, up-regulation in GLUT-1 transporters and glycolytic enzymes was first associated with HIF-1α stabilization (Robey *et al*., 2008). Recently, other, HIF-1α-independent pathways have been implicated in direct up-regulation of glycolysis, such as c-Myc (Robey *et al*., 2008) and PI3K/AKT/mTOR pathways (Plas and Thompson, 2005). BCR-ABL directly up-regulates the PI3K/AKT/mTOR pathway (Kim *et al*., 2005) and leads to induction of glycolysis in CML cells followed by increased cell proliferation. This can be inhibited by the BCR-ABL tyrosine kinase inhibitor imatinib in sensitive, but not in the resistant cells.

As previously reported (Mahon *et al*., 2000; Donato *et al*., 2003), the resistant cell lines K562-r, K562-R and LAMA84-r have different levels of expression of the Bcr-Abl oncoprotein. Due to their different mechanisms of resistance, differences in cell metabolism were also found in K562-r versus LAMA84-r cell lines. This includes differences in high-energy phosphate metabolism and the mitochondrial TCA cycle. In addition, differences in Pgp expression among resistant cells were also observed. The LAMA84-r cells markedly overexpressed Pgp; K562-r (1 μM) had only a slight elevation in Pgp expression, while K562-R (5 μM) showed no changes in Pgp expression. The K562-r (1 μM) and LAMA84-r had decreased intracellular imatinib concentrations. This may be one of the reasons for their resistance to imatinib. A number of metabolic studies with wild-type and MDR1 overexpressing resistant cell lines have been reported. Overexpressing resistant cells have been found to have an increased glycolysis rate (Lyon *et al*., 1988) and elevated levels of NTP (Kaplan *et al*., 1990).

Nonetheless, despite their distinct mechanisms of imatinib resistance, there were similarities in the metabolic profiles of both K562-r and LAMA84-r cells. The metabolic pathways that were identical in all three resistant cell lines, were: (i) increased phospholipid PC/GPC ratios; and (ii) increased glycolytical activities when compared with sensitive cells. These two metabolic pathways were characteristic for resistance development (maintenance of high proliferation rate and lack of apoptosis), regardless of the mechanism of resistance induction, Pgp overexpression and/or intracellular imatinib concentrations.

In conclusion, these findings may provide the basis for early detection of patients developing resistance to imatinib (with various molecular aberrations in BCR-ABL signalling) using a metabolic profiling of blood samples. Metabolic changes in cancer metabolism, such as those described here, often occur before clinical manifestations of disease progression (increase in the blood cell count), as has been shown for solid c-kit-positive tumours resistant to imatinib, in clinical positron emission tomography studies (Grimpen *et al*., 2005). Therefore, metabolic NMR assessment of phospholipid and glucose pathways in blood cells from imatinib-treated patients may have the potential to detect the development of resistance at early stages and follow-up on effectiveness of alternative therapies.

Acknowledgements

The study was supported by the National Cancer Institute, grants R21CA108624 (NJS, SGE, JMK, DJK, JLB) and P30CA046934 (NJS, DJK, JLB). We thank Dr Moshe Talpaz (M.D. Anderson Cancer Center) for providing us with K562-r (5μM) cells and Dr Elisabeth Buchdunger (Novartis Pharma AG) for the supply of imatinib and helpful discussions.

Conflicts of interest

None.

References

Barnes K, McIntosh E, Whetton AD, Daley GQ, Bentley J, Baldwin SA (2005). Chronic myeloid leukaemia: an investigation into the role of Bcr-Abl-induced abnormalities in glucose transport regulation. *Oncogene* **24**: 3257–3267.

Boren J, Cascante M, Marin S, Comin-Anduix B, Centelles JJ, Lim S *et al*. (2001). Gleevec (STI571) influences metabolic enzyme activities and glucose carbon flow toward nucleic acid and fatty acid synthesis in myeloid tumor cells. *J Biol Chem* **276**: 37747–37753.

Boros LG, Cascante M, Lee WN (2002). Metabolic profiling of cell growth and death in cancer: applications in drug discovery. *Drug Discov Today* **7**: 364–372.

Buchdunger E, Zimmermann J, Mett H, Meyer T, Muller M, Druker BJ *et al*. (1996). Inhibition of the Abl protein-tyrosine kinase in vitro and in vivo by a 2-phenylaminopyrimidine derivative. *Cancer Res* **56**: 100–104.

Buchdunger E, Cioffi CL, Law N, Stover D, Ohno-Jones S, Druker BJ *et al*. (2000). Abl protein-tyrosine kinase inhibitor STI571 inhibits in vitro signal transduction mediated by c-kit and platelet-derived growth factor receptors. *J Pharmacol Exp Ther* **295**: 139–145.

le Coutre P, Tassi E, Varella-Garcia M, Barni R, Mologni L, Cabrita G *et al*. (2000). Induction of resistance to the Abelson inhibitor STI571 in human leukemic cells through gene amplification. *Blood* **95**: 1758–1766.

Deininger MW, Goldman JM, Lydon N, Melo JV (1997). The tyrosine kinase inhibitor CGP57148B selectively inhibits the growth of BCR-ABL-positive cells. *Blood* **90**: 3691–3698.

Deininger MW, Goldman JM, Melo JV (2000). The molecular biology of chronic myeloid leukemia. *Blood* **96**: 3343–3356.

Desplat V, Belloc F, Lagarde V, Boyer C, Melo JV, Reiffers J *et al*. (2005). Overproduction of BCR-ABL induced apoptosis in imatinib-mesylate resistant cell lines. *Cancer* **103**: 102–110.

Donato NJ, Wu JY, Stapley J, Gallick G, Lin H, Arlinghaus R *et al*. (2003). BCR-ABL independence and LYN kinase overexpression in chronic myelogenous leukemia cells selected for resistance to STI571. *Blood* **101**: 690–698.

Druker BJ, Tamura S, Buchdunger E, Ohno S, Segal GM, Fanning S *et al*. (1996). Effects of a selective inhibitor of the Abl tyrosine kinase on the growth of Bcr-Abl positive cells. *Nat Med* **2**: 561–566.

Evelhoch JL, Gillies RJ, Karczmar GS, Koutcher JA, Maxwell RJ, Nalcioglu O *et al*. (2000). Applications of magnetic resonance in model systems: cancer therapeutics. *Neoplasia* **2**: 152–165.

Franks SE, Smith MR, Arias-Mendoza F, Shaller C, Padavic-Shaller K, Kappler F *et al*. (2002). Phosphomonoester concentrations differ between chronic lymphocytic leukemia cells and normal human lymphocytes. *Leuk Res* **26**: 919–926.

Gambacorti-Passerini C, le Coutre P, Mologni L, Fanelli M, Bertazzoli C, Marchesi E *et al*. (1997). Inhibition of the ABL kinase activity blocks the proliferation of BCR/ABL+ leukemic cells and induces apoptosis. *Blood Cells Mol Dis* **23**: 380–394.

Glunde K, Serkova NJ (2006). Therapeutic targets and biomarkers identified in cancer choline phospholipid metabolism. *Pharmacogenomics* **7**: 1109–1123.

Gorre ME, Mohammed M, Ellwood K, Hsu N, Paquette R, Rao PN *et al*. (2001). Clinical resistance to STI-571 cancer therapy caused by BCR-ABL gene mutation or amplification. *Science* **293**: 876–880.

Gottschalk S, Anderson N, Hainz C, Eckhardt SG, Serkova NJ (2004). Imatinib (STI571)-mediated changes in glucose metabolism in human leukemia BCR-ABL-positive cells. *Clin Cancer Res* **10**: 6661–6668.

Grimpen F, Yip D, McArthur G, Waring P, Goldstein D, Loughrey M *et al*. (2005). Resistance to imatinib, low-grade FDG-avidity on PET, and acquired KIT exon 17 mutation in gastrointestinal stromal tumour. *Lancet Oncol* **6**: 724–727.

Henke J, Engelmann J, Kutscher B, Nessner G, Engel J, Voegeli R *et al*. (1999). Changes of intracellular calcium, fatty acids and phospholipids during miltefosine-induced apoptosis monitored by fluorescence- and 13C NMR-spectroscopy. *Anticancer Res* **19**: 4027–4032.

Jordanides NE, Jorgensen HG, Holyoake TL, Mountford JC (2006). Functional ABCG2 is overexpressed on primary CML CD34+ cells and is inhibited by imatinib mesylate. *Blood* **108**: 1370–1373.

Kaplan O, van Zijl PC, Cohen JS (1990). Information from combined ^{1}H and ^{31}P NMR studies of cell extracts: differences in metabolism between drug-sensitive and drug-resistant MCF-7 human breast cancer cells. *Biochem Biophys Res Commun* **169**: 383–390.

Kim JH, Chu SC, Gramlich JL, Pride YB, Babendreier E, Chauhan D *et al*. (2005). Activation of the PI3K/mTOR pathway by BCR-ABL contributes to increased production of reactive oxygen species. *Blood* **105**: 1717–1723.

Klawitter J, Schmitz V, Klawitter J, Leibfritz D, Christians U (2007). Development and validation of an assay for the quantification of 11 nucleotides using LC/LC-electrospray ionization-MS. *Anal Biochem* **365**: 230–239.

Klawitter J, Zhang YL, Klawitter J, Anderson N, Serkova NJ, Christians U (2009). Development and validation of a sensitive assay for the quantification of imatinib mesylate using LC/LC-MS/MS in blood and cell culture. *J Chromatogr B Biomed Sci Appe* (in press).

Lyon RC, Cohen JS, Faustino PJ, Megnin F, Myers CE (1988). Glucose metabolism in drug-sensitive and drug-resistant human breast cancer cells monitored by magnetic resonance spectroscopy. *Cancer Res* **48**: 870–877.

Mahon FX, Deininger MW, Schultheis B, Chabrol J, Reiffers J, Goldman JM *et al*. (2000). Selection and characterization of BCR-ABL positive cell lines with differential sensitivity to the tyrosine kinase inhibitor STI571: diverse mechanisms of resistance. *Blood* **96**: 1070–1079.

Melo JV, Chuah C (2007). Resistance to imatinib mesylate in chronic myeloid leukaemia. *Cancer Lett* **249**: 121–132.

Morse DL, Carroll D, Day S, Gray H, Sadarangani P, Murthi S *et al*. (2009). Characterization of breast cancers and therapy response by MRS and quantitative gene expression profiling in the choline pathway. *NMR Biomed* **22**: 114–127.

Plas DR, Thompson CB (2005). Akt-dependent transformation: there is more to growth than just surviving. *Oncogene* **24**: 7435–7442.

Robey IF, Stephen RM, Brown KS, Baggett BK, Gatenby RA, Gillies RJ (2008). Regulation of the Warburg effect in early-passage breast cancer cells. *Neoplasia* **10**: 745–756.

Roche-Lestienne C, Soenen-Cornu V, Grardel-Duflos N, Lai JL, Philippe N, Facon T *et al*. (2002). Several types of mutations of the Abl gene can be found in chronic myeloid leukemia patients resistant to STI571, and they can pre-exist to the onset of treatment. *Blood* **100**: 1014–1018.

Serkova N, Boros LG (2005). Detection of resistance to imatinib by metabolic profiling: clinical and drug development implications. *Am J Pharmacogenomics* **5**: 293–302.

Serkova N, Fuller TF, Klawitter J, Freise CE, Niemann CU (2005). ^{1}H-NMR based metabolic signatures of mild and severe ischemia/reperfusion injury in rat kidney transplants. *Kidney Int* **67**: 1142–1151.

Thomas J, Wang L, Clark RE, Pirmohamed M (2004). Active transport of imatinib into and out of cells: implications for drug resistance. *Blood* **104**: 3739–3745.

Van Etten RA (2004). Mechanisms of transformation by the BCR-ABL oncogene: new perspectives in the post-imatinib era. *Leuk Res* **28**: S21–S28.

Warburg O (1956). On the origin of cancer cells. *Science* **123**: 309–314.

Wu J, Meng F, Lu H, Kong L, Bornmann W, Peng Z *et al*. (2008). Lyn regulates BCR-ABL and Gab2 tyrosine phosphorylation and c-Cbl protein stability in imatinib-resistant chronic myelogenous leukemia cells. *Blood* **111**: 3821–3829.

Zamaraeva MV, Sabirov RZ, Maeno E, Ando-Akatsuka Y, Bessonova SV, Okada Y (2005). Cells die with increased cytosolic ATP during apoptosis: a bioluminescence study with intracellular luciferase. *Cell Death Differ* **12**: 1390–1397.

Zhou R, Vander Heiden MG, Rudin CM (2002). Genotoxic exposure is associated with alterations in glucose uptake and metabolism. *Cancer Res* **62**: 3515–3520.

Zwingmann C, Leibfritz D (2003). Regulation of glial metabolism studied by 13C-NMR. *NMR Biomed* **16**: 370–399.